Journal of Ceramic Processing Research. Vol. 23, No. 2, pp. 237~242 (2022)
(Received 23 February 2022, Received in revised form 13 April 2022, Accepted 13 April 2022)
https://doi.org/10.36410/jcpr.2022.23.2.237

J O U R N A L O F
Ceramic Processing Research

Effect of La_2O_3 upon optical properties of oxy-fluoride glasses

Taewan Ha and Seunggu Kang*
Department of Advanced Materials Science and Engineering, Kyonggi University, Suwon, Korea

In this paper, the bonding states between composition ions and changes in the optical properties of glass according to the amount of substitution of La_2O_3 in La_2O_3-CaF_2-Al_2O_3-SiO_2 glass (hereinafter referred to as LCAS glass system) were studied. By analyzing the molar volume, density, and number of chemical bonds per unit volume of LCAS glass, it was confirmed that the added La_2O_3 acted as a glass network modifier. As the amount of substitution of La_2O_3 increased, the numbers of non-bridging oxygen and electron polarization increased, thereby reducing the optical band gap of the glass. As a result, it was confirmed that semiconducting behavior was exhibited in the glass. The La_2O_3-CaF_2-Al_2O_3-SiO_2 glass prepared in this study had a light transmittance of 75% or more, and the optical band gap energy could be changed as a function of amount of La_2O_3 substitution. It is concluded that LCAS glass can be used in various optical device fields such as optical sensors and lasers by controlling the amount of La_2O_3 substitution.

Keywords: La_2O_3, Modifier, Optical band gap, Oxy-fluoride glasses.

Introduction

In general, glass is manufactured by melting an oxide powder at a high temperature and then exposing it to the room temperature atmosphere for rapid cooling. The properties of glass are mainly affected by the bond type and strength of constituent atoms. Therefore, many researches have been performed to control the structure and properties of glass by controlling the numbers of bridging oxygen and non-bridging oxygen by adding an intermediate and a modifier to the glass former oxides [1-4].

Among studies cited above, interest in optical glass with capability of controlling optical properties by changing the phonon energy of the structural lattices has recently been increasing. Examples of application of optical glass to high-tech industrial fields include displays, lasers, optical fiber, and biomedical devices [5-11].

Alumino-silicate glass has excellent chemical durability and mechanical stability due to the excellent glass-forming ability of Al^{3+} and Si^{4+} cations among constituent ions. In addition, owing to the advantage of high transmittance to visible light, it has been utilized in various fields [12-16]. However, due to the high phonon energy of the Si-O-Si bond, when ions of rare earth and transition metals are added to glass, the luminous efficiency is low, and thus there is a limitation in application to optical fibers and laser materials.

*Corresponding author:
Tel : +82-31-249-9767
Fax: +82-31-249-9774
E-mail: sgkang@kyonggi.ac.kr

On the other hand, oxy-fluoride glass has the advantage that high luminous efficiency can be expected due to low phonon energy. However, the disadvantage of oxy-fluoride glass is that it has low chemical durability. Recently, as improved luminous efficiency as well as durability by precipitating fluoride-based crystals on an oxide glass matrix is known, research on oxy-fluoride glass is rapidly progressing [17]. When a rare-earth material is doped into an oxy-fluoride glass, a specific electron transition occurs depending on the type of ion of the rare-earth element, and the glass will thereby emit a specific wavelength [18].

The luminescence of rare earth ions is caused by electrons in the 4f orbital, but there are no electrons in the 4f orbital of the La^{3+} ion in La_2O_3. However, due to the high field strength of La^{3+} ion , there is a possibility of exhibiting high-quality luminescence intensity, and numerous studies on fluoride glass systems with added La_2O_3 thus have been conducted recently. In addition, since La_2O_3 has a high refractive index (2.0-2.3) and Abbe number, it lowers the optical aberration of the glass. Therefore, when used as an optical device lens, an image is formed accurately. Moreover, the band gap change can be controlled according to the composition, facilitating use in various optical materials.

Elkhoshkhany et al. [19] and Goel et al. [20] studied changes in the structure and the optical properties by adding La_2O_3 to zinc-tellurite glass and silicate glass, respectively. Although many researches have been conducted on the effects of La^{3+} ions on glass of various compositions, relatively few studies on oxy-fluoride glass have been reported. In this light, in this paper, the effect of La_2O_3 substitution on the structure and the optical properties of CaF_2-Al_2O_3-SiO_2 glass, which is

an oxy-fluoride-based glass, was studied.

Experimental

As starting materials for oxy-fluoride glass production, CaF_2 (99.9%), α-Al_2O_3 (99.9%), SiO_2 (99.9%), and La_2O_3 (99.9%) were used. The batches of La_2O_3-CaF_2-Al_2O_3-SiO_2 glass prepared in this experiment is shown in Table 1. The batch prepared as powder was mixed for 24 h, put in a platinum crucible, and melted at 1450 °C for 1 h. The obtained melt then was formed into a graphite mold of cylinder form and annealed at 400 °C for 1 h to prepare a glass from which stress was removed.

The density of the manufactured LCAS glass was measured using principle of Archimedes, and the molar volume of glass was also calculated through the measured density value. The formulas for density and molar volume are as follows:

$$\rho = \frac{W}{V} \tag{1}$$

$$V_M = \frac{M}{\rho} = \frac{\sum(x_i \cdot M_i)}{\rho} \tag{2}$$

In Eq. (1), ρ is the specimen's density (g/cm^3), V is the volume of the glass specimen (cm^3), and W is the weight of the specimen in air (g). In Eq. (2), V_M is the molar volume (cm^3/mol) of the glass specimen, M is the molar mass (g/mol) of the glass specimen, x_i is the mole fraction of each molecule, and M_i is the molecular weight of each molecule. The crystalline phase generated in the prepared glass was confirmed using an x-ray diffraction analysis. For measurement of the light transmittance and absorbance, the glass was polished to a thickness of 3mm or less, and an ultraviolet-visible spectrophotometer was used. The refractive index of glass at a wavelength of 589 nm was obtained with an Abbe refractometer (ATAGO 2T, ATAGO CO., LTD. Japan).

Results and Discussion

Among the properties of glass, density and molar volume are structural parameters and are closely related to factors indicating the degree of densification of the glass structure, the coordination number, and the presence or absence of internal pores [21-22]. The density of the glass increased linearly from 2.74 to 3.00 (g/cm^3) as the amount of La_2O_3 substitution was increased, as shown in Fig. 1. This is because, as La_2O_3 (325.81 g/mol), having a heavier atomic weight than SiO_2 (60.09 g/mol), was added, the density of the glass specimen was increased. In addition, the molar volume (V_M) of the glass increased with the amount of La_2O_3 substitution. La_2O_3 is known to act as a modifier when added to oxide-silicate glass [23]. Therefore, it is thought that the numbers of non-bridging oxygen increased with the amount of La_2O_3 added, and V_M also increased because the glass-network structure was opened accordingly [24].

Table 1. Composition of LCAS glass system fabricated in this study (mol%)

Sample I.D.	SiO_2	Al_2O_3	CaF_2	La_2O_3
La0	50	20	30	0
La1	49	20	30	1
La2	48	20	30	2
La3	47	20	30	3

The number of bonds per volume (n_b) in glass is a factor showing the bonding properties of glass and can be obtained through the following equation [25]:

$$n_b = \frac{N_A}{V_M} \cdot \sum(x_i \cdot n_c) \tag{3}$$

In Eq. (3), N_A is number of Avogadro, n_c is the coordination number of the cation, and x_i is the mole fraction of each composition. Elkhoshkhany et al. studied the change of the ion radius, the numbers of oxygen displaced, and the glass network according to the NaF substitution amount in oxy-fluoride glass. As a result, it was found that Na^+ ions act as modifiers and decrease the number of bond per unit volume [26].

The number of bonds (n_b) per unit volume of glass with the amount of La_2O_3 addition is shown in Fig. 2. n_b decreased with amount of La_2O_3 substituted, which means that the network connectivity decreased and the glass network was loosened. Therefore, it was confirmed that La_2O_3 acted as a modifier for generating non-bridging oxygen in the network structure of glass. This was consistent with the analysis results of V_M shown in Fig. 1. Fig. 3 shows the results of the XRD analysis for LCAS glass specimen. Sharp peaks representing specific crystals did not appear and only large hill-shaped peaks were noted. Therefore, all glass specimens have an amorphous structure, and it appears that only 0-3 mol% La_2O_3 substitution does not produce crystals in the glass.

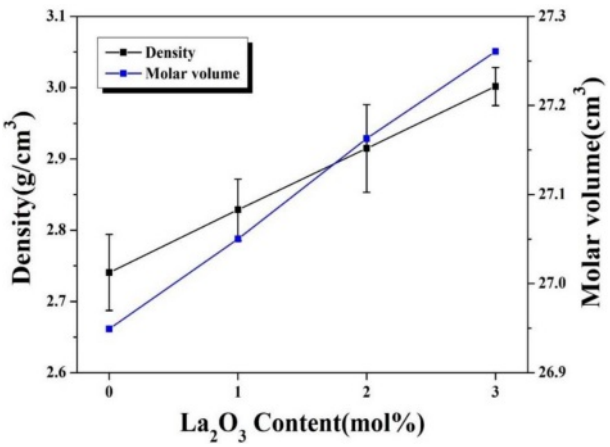

Fig. 1. Density and volume per mole of LCAS glass system as a function of amount of La_2O_3 substituted.

In order to analyze the correlation between the bonding state and optical properties of the glass network, the polarizability, which has a close relationship with the electron transition, was calculated. The polarizability can be obtained using the Lorentz-Lorenz equation as follows [26]:

$$R_m = \left[\frac{n^2-1}{n^2+2}\right] \cdot \frac{M}{\rho} = \left[\frac{n^2-1}{n^2+2}\right] \cdot V_M \quad (4)$$

$$\alpha_m = \left(\frac{3}{4\pi N_A}\right) \cdot R_m \quad (5)$$

$$\alpha_{anion} = \frac{\left[\frac{R_m}{2.52} - \sum \alpha_{cation}\right]}{N_{anion}} \quad (6)$$

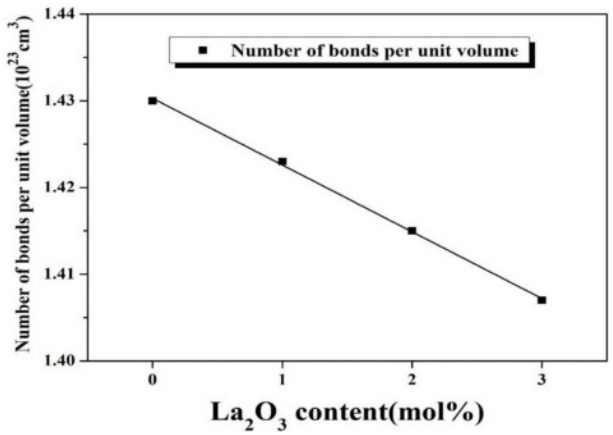

Fig. 2. Number of bonds in volume unit of LCAS glass system as a function of amount of La_2O_3 substituted.

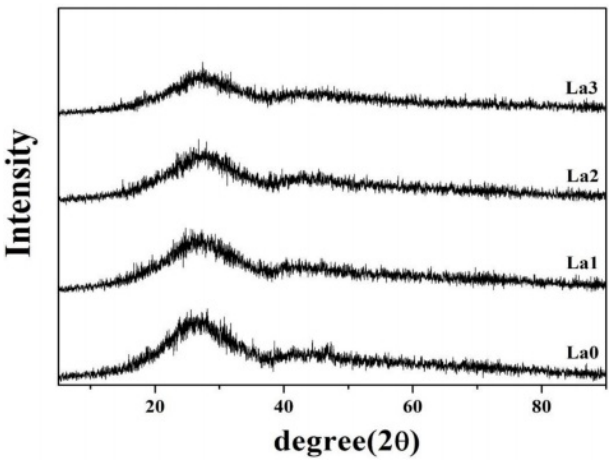

Fig. 3. XRD patterns of LCAS glass system according to amount of La_2O_3 substituted.

In Eq. (4), R_m is the total molar refraction of the material and n is the refractive index. In Eq. (5), α_m denote the molar polarizability of electron. In formula (6), α_{anion} is the electronic polarizability of the anions (O^{2-} and F^-). N_{anion} means the total number of anions constituting the glass composition, and $\sum\alpha_{cation}$ is the molar cation polarizability of the cations. In previously published studies, α_{Si} = 0.033Å^3, α_{Al} = 0.054Å^3, α_{La} = 1.052Å^3, and α_{Ca} = 0.68Å^3 were measured [27-29]. Table 2 shows the molar refraction, refractive index, electronic polarizability, and molar cation polarizability of the LCAS glass prepared in this study. As the amount of substitution of La_2O_3 increases, the refractive index increases. This can be interpreted as a simple rule of the mixture phenomenon that occurs because La_2O_3 is substituted for SiO_2 with a low refractive index. The value of α_m increases with the amount of La_2O_3 substituted, because the electron polarization of the La^{3+} cation is higher than that of Si^{4+}. Therefore, it is considered that the substituted La^{3+} cations contributed in part to the glass refractive index increase. In addition, as the amount of substitution of La_2O_3 increased, the electron polarization of the anion increased, which is expected to facilitate electron transition [30-34].

Fig. 4 shows the light transmittance of the glass with La^{3+} cation substitution. When 1 to 2 mol% of La^{3+} was substituted, the light transmittance in the range of 400 to 800 nm decreased slightly from 91% to 88%, but when 3 mol% was added, it decreased sharply to 75%. Cetinkaya et al. observed the change in light transmittance according to the amount of ZnO added, and explained

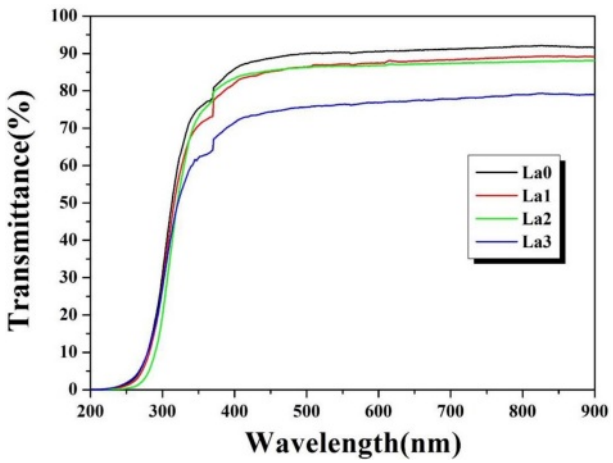

Fig. 4. Transmittance graph of LCAS glass system as a function of an amount of La_2O_3 substituted.

Table 2. Refraction–related properties of LCAS glass system according to amount of La_2O_3 substituted

Properties	La0	La1	La2	La3
Refractive index (at 589 nm)	1.54	1.64	1.66	1.67
Molar refraction, R_m (cm^3/mol)	8.46	9.75	10.03	10.18
Molar electronic polarizability, α_m (Å^3)	3.35	3.86	3.98	4.04
Electronic polarizability of anion, α_{anion} (Å^3)	1.42	1.63	1.67	1.68

that the light transmittance of glass decreased because ZnO acted as a modifier and the numbers of non-bridging oxygen increased [27]. Therefore, it is thought that the light transmittance of the glass prepared in this study also decreased as the numbers of non-bridging oxygen increased due to La^{3+}.

Fig. 5 shows the absorbance graph with La^{3+} cation substitution of the glass prepared in this study. When the La_2O_3 substituted specimen and the unsubstituted specimen were compared, a very similar pattern was observed over all wavelength bands. Also, the absorption edge can be obtained from the point where the tangent line drawn on the absorbance graph meets the wavelength axis. Table 3 shows the calculated absorption edge of the LACS glass. As the amount of substitution of La^{3+} cations increased, the absorption edge showed a tendency to shift to a longer wavelength band. This result is consistent with the results of research by Guo et al. showing that the absorption edge of mother glass shifts to a long wavelength band depending on the doping amount of Tb^{3+}, a rare earth ion [32]. Guo et al. attributed this to Tb_2O_3 acting as a modifier to generate non-bridging oxygen. In other words, the absorption edge shifted toward longer wavelength because the non-bridging oxygen showed more polarization than the bridging oxygen. Therefore, it can be considered that the La^{3+} ions added to the glass prepared in this experiment also acted as modifiers.

Glassy materials do not show the long-range order that is a typical of crystalline solids with a periodic potential. The short range order in glassy materials, however, remains to some extent, causing to happen, thereby to a band-like structure of electron energy states comparable to that of crystalline solids. The localized electron levels occur near the band edges at somewhat high densities of state tailing into the band gap, called as diffuse band tail states. The direct and indirect optical transitions, which occurs at the absorption edge of non-crystalline materials. Glassy materials are often associated with a band tailing of density of states [33].

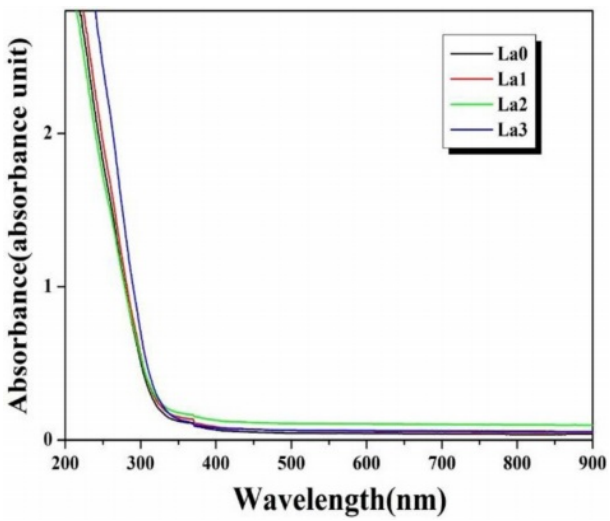

Fig. 5. Absorbance graph of LCAS glass system according to amount of La_2O_3 substituted.

Table 3. Absorption edge of LCAS glass system as a function of amount of La_2O_3 substituted.

Optical Properties	La0	La1	La2	La3
Absorption edge(nm)	318	321	326	334

Mott and Davis suggested that the optical band gap according to the transition can be obtained from the following eq. (7): [33]

$$\alpha = \frac{\alpha_0 (hv - E_g{}^{opt})^n}{hv} \quad (7)$$

In Eq. (7), when the value of n, the exponent, is 1/2, it means an allowed direct transition, and when it is 2, it means an allowed indirect transition. Here, α is the absorption coefficient, α_0 is a constant, and $E_g{}^{Opt}$ is the optical band gap. In addition, the absorption coefficient α can be obtained by substituting the absorbance A and the specimen thickness d in the following eq. (8) [31]:

$$\alpha = 2.303 \times \frac{A}{d} \quad (8)$$

From the $(\alpha hv)^n$ versus hv graph drawn using Eq. (7), the optical band gap (E_g^{Opt}) could be calculated when the $(\alpha hv)^n$ (n=1/2 or 2) value is 0. [31] Fig. 6 shows a graph of $(\alpha hv)^n$ (n=1/2 or 2) according to the energy of the wavelength, that is, the phonon energy (hv). The graphs in Figs. 6(a) and (b) are for n=1/2 and n=2, respectively. In each figure, when the $(\alpha hv)^n$ value is 0 by extrapolation, E_g^{Opt} is obtained. In (a), the direct optical band gap is obtained, and in (b), the indirect optical band gap is obtained. The band gap values of LCAS glass obtained in this manner are shown in Table 4. Both the direct band gap and indirect band gap decreased as the amount of La_2O_3 substitution increased.

One of several factors that can indirectly determine the degree of electron transition is the electron polarization of an anion [34]. Fig. 7 shows the relationship between the electron polarization of anions and the band gap in LCAS glass. As the amount of substitution of La_2O_3 increased, the electron polarization of anions rapidly increased from 1.41 to 1.63. In addition, as the anion electron polarizability increased, both the direct band gap and the indirect band gap decreased, and the direct band gap was always higher than the indirect band gap in all specimens.

The reason for this is, first, the La^{3+} cation in the glass acts as a glass modifier, increasing the numbers

Table 4. Band gaps of LCAS glass system as a function of amount of La_2O_3 substituted.

Parameter	La0	La1	La2	La3
Direct band gap(eV)	4.53	4.34	4.30	4.22
Indirect band gap(eV)	3.94	3.88	3.85	3.83

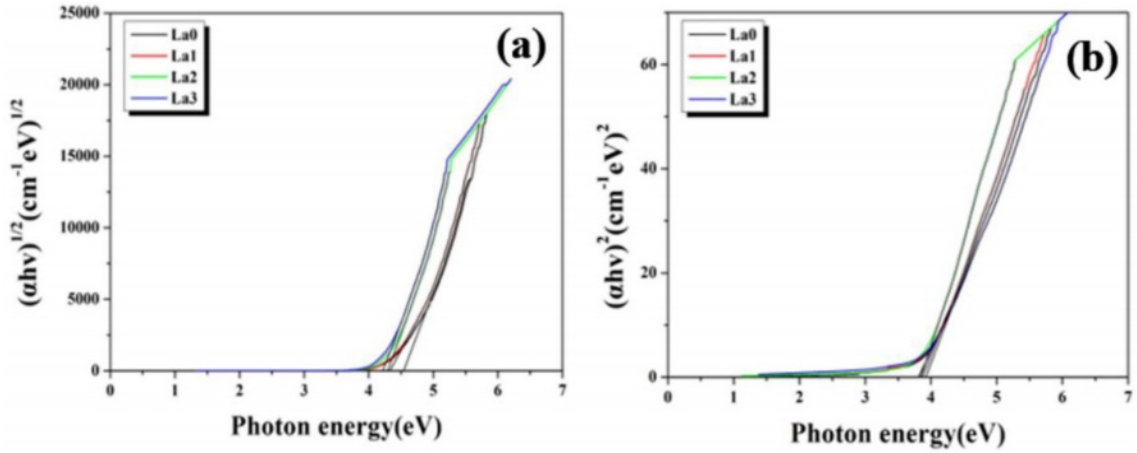

Fig. 6. Photon energy vs. (a) $(\alpha hv)^{1/2}$ and (b) $(\alpha hv)^2$ graph of LCAS glass system according to amount of La_2O_3 substituted.

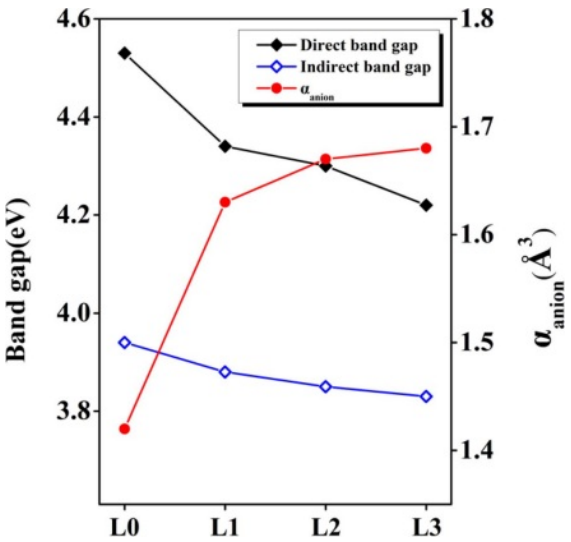

Fig. 7. Direct band gap, indirect band gap, and electronic polarizability of anions of LCAS glass system according to amount of La_2O_3 substituted.

of non-bridging oxygen that facilitate the optical electron transition. Second, as the amount of La^{3+} substitution increased, the electron polarization of anions increased. Therefore, it can be seen that the optical bandgap can be controlled by adjusting the amount of La^{3+} ions added to the LCAS mother glass prepared in this study [35-36].

Conclusions

In this study, CaF_2-Al_2O_3-SiO_2 based mother glass was prepared and its optical properties according to the change in the bonding states of the glass structure were analyzed as a function of amount of La_2O_3 substitution. The density increased with the amount of La_2O_3 substitution, but the molar volume (V_M) and the number of bonds in volume unit (n_b) decreased, indicating that La^{3+} ions acted as modifiers. The light transmittance of the glass decreased with the amount of La_2O_3 substitution. From the absorbance results, it was confirmed that La^{3+} ions increased non-bridging oxygen, which caused a difference in the polarization of electrons, and that the absorption edge moved toward the long wavelength.

As the amount of La_2O_3 substitution increased, both the direct band gap and the indirect band gap decreased. This is thought to be attributable to the optical transition becoming easier due to the increased numbers of non-bridging oxygen and the increase in the electron polarization of anions. The La_2O_3-CaF_2-Al_2O_3-SiO_2 glass prepared in this study shows more than 75% transparency and the value of optical band gap energy can be controlled as a function of amount of La_2O_3 substitution. Therefore, it could be applicable to various devices for optics such as optical sensors and lasers. However, it is necessary to additionally conduct research on crystal growth control of LCAS-based glass, and changes in bonding structure and optical properties due to crystallization.

Acknowledgement

This work was supported by Kyonggi University Research Grant 2019.

References

1. A. Novatski, A. Steimacher, A.N. Medina, A.C. Bento, M.L. Baesso, L.H.C. Andrade, S.M. Lima, Y. Guyot, and G. Boulon, J. Appl. Phys. 104[9] (2008) 094910.
2. M.L.F. Nascimento and N.O. Dantas, Mater. Lett. 61 (2007) 912-916.
3. M.M. Hivrekar, D.B, Sable, M.B. Solunke, and K.M. Jadhav, J. Non-Cryst. Solids. 474 (2017) 58-65.
4. Z. Luo, J. Zhang, J. Liu, J. Song, and A. Lu, Solid State Ionics, 317 (2018) 76-82.
5. G. Hou, C. Zhang, W. Fu, G. Li, J. Xia, and Y. Ping, Ceram. Int. 45 (2019) 11850-11855.
6. Q. Zhang, L. Han, W. Liu, W. You, A. Lu, and Z. Luo, J. Ceram. Process. Res. 22[1] (2021) 8-15.

7. Y. Zhang, Z. Zhang, X. Liu, G. Shao, L. Shen, J. Liu, W. Xiang, and X. Liang, Chem. Eng. J. 401 (2020) 125983.
8. J. Lei, Q. Zhang, Y. Song, J. Tang, J. Tong, F. Peng, and H. Xiao, Opt. Laser Technol. 128 (2020) 106223
9. S. Kaewjaeng, S. Kothan, W. Chaiphaksa, N. Chanthima, R. Rajaramakrishna, H.J. Kim, and J. Kaewkhao, Radiat. Phys. Chem. 160 (2019) 41-47.
10. D. Shiratori, Y. Isokawa, H. Samizo, M. Koshimizu, N. Kawaguchi, and T. Yanagida, J. Ceram. Process. Res. 20[4] (2019) 301-306.
11. G. Okada, H. Masai, A. Torimoto, S. Kasap, and T. Yanagida, J. Ceram. Process. Res. 17[3] (2016) 148-151.
12. P.R. Watekar, S.M. Ju, S.J. Boo, and W.T. Han, J. Non-Cryst. Solids. 351 (2005) 2446-2452.
13. P.R. Watekar, S.M. Ju, and W.T. Han, Colloids Surf. A Physicochem. Eng. Asp. 313-314 (2008) 492-496.
14. A. Halder, M.C. Paul, S.W. Harun, S.K. Bhadra, S. Bysakh, and S. Das, M. Pal, J. Lumin. 143 (2013) 393-401.
15. A. Ashjari, B.E. Yekta, and H.R. Rezaie, J. Eur. Ceram. Soc. 40 (2020) 1368-1375.
16. N. Suebsing, C. Bootjomchai, V. Promarak, and R. Laopaiboon, J. Non-Cryst. Solids. 523 (2019) 119598.
17. M. Li, J. Zou, G. Guo, J. Liu, and G. Wang, J. Ceram. Process. Res. 22[5] (2021) 504-509.
18. D. Nakauchi, M. Koshimizu, N. Kawaguchi, and T. Yanagida, J. Ceram. Process. Res. 20[4] (2019) 307-313.
19. N. Elkhoshkhany, R. Essam, and E.S. Yousef, J. Non-Cryst. Solids. 536 (2020) 119994,
20. A. Goel, D.U. Tulyaganov, V.V. Kharton, A.A. Yaremchenko, and J.M.F. Ferreira, Acta Mater. 56 (2008) 3065-3076.
21. Z. Shen, Y. Zhao, Z. Tian, W. Huang, J. Wu, and H. Lin, J. Non-Cryst. Solids. 499 (2018) 17-24.
22. I. Kashif, A.A. El-Maboud, and A. Ratep, Results Phys. 4 (2014) 1-5.
23. A.K. Varshneya and J.C. Mauro, "Fundamentals of Inorganic Glasses" (Elsevier, 2019) p.1.
24. A. Gaddam, H.R. Fernandes, D.U. Tulyaganov, and J.M.F. Ferreira, J. Non-Cryst. Solids. 505 (2019) 18-27.
25. M. Abdel-Baki, F.A. Abdel-Wahab, and F. El-Diasty, J. Appl. Phys. 111 (2012) 073506.
26. N. Elkhoshkhany, M. Mahmoud, and E. Sayed-Yousef, Chalcogenide Lett. 16[6] (2019) 265-282.
27. Y.B. Saddeek, K.A. Aly, and S.A. Bashier, Physica B 405 (2010) 2407-2412.
28. M.K. Halmah, M.F. Faznny, M.N. Azlan, and H.A.A. Sidek, Results Phys. 7 (2017) 581-589.
29. R.D. Shannon, and R.X. Fischer, Am. Mineral. 101[10] (2016) 2288-2300.
30. S.C. Colak, I. Akyuz, and F. Atay, J. Non-Cryst. Solids. 432 (2016) 406-412.
31. A.H. Hammad, M.A. Marzouk, and H.A. El-Batal, Silicon 8 (2016) 123-131.
32. H. Guo, Y. Wang, Y. Gong, H. Yin, Z. Mo, Y. Tang, and L. Chi, J. Alloys Compd. 686 (2016) 635-640.
33. E.A. Davis, and N.F. Mott, Philos. Mag. 22[179] (1970) 903-922.
34. Z.A.S. Mahraz, M.R. Sahar, and S.K. Ghoshal, J. Mol. Struct. 1072 (2014) 238-241.
35. A. Herrmann, M. Tewelde, S. Kuhn, M. Tiegel, and C. Rüssel, J. Non-Cryst. Solids. 502 (2018) 190-197.
36. R.S. Gedam, and D.D. Ramteke, J. Phys. Chem. Solids. 74 (2013) 1039-1044.